

Origins of Thixotropy

Leslie V. Woodcock

*Schools of Chemical Engineering, University of Bradford, Bradford,
West Yorkshire BD7 1DP, United Kingdom*

(Received 21 August 1984)

Soft-sphere scaling laws and nonequilibrium particle-dynamics simulations show that time-dependent shear-thinning behavior involving structural ordering (thixotropy), typically seen in complex colloidal dispersions, derives from a first-order thermodynamic phase transition between a normal shearing fluid and a partially ordered smectic phase. The transition stems from a perturbation of the equilibrium fluid freezing point by the applied strain rate.

PACS numbers: 64.70.Ew, 05.70.Ln

The scaling laws of soft spheres, defined by the model pair potential

$$\phi(r) = \epsilon(\sigma/r)^n, \quad (1)$$

provide unique insight into equations of state and phase diagrams,¹ melting and freezing,² glass transition phenomena,³ self-diffusion,⁴ and the transport coefficients of viscous flow and thermal conductance,⁵ correlating diverse molecular-fluid properties over whole p - V - T ranges. This singular success of the soft-sphere model arises because all these phenomenological properties share a common geometric origin at the particulate level. The underlying determining structures, and the statistical fluctuations of those structures, depend primarily on the repulsive part of an effective pairwise additive potential well approximated by Eq. (1).

Non-Newtonian flow curves for a range of sheared colloidal suspensions including both the characteristic shear-thinning and shear-thickening (dilatant) regions have recently been found to conform closely to the flow curve calculated for a soft-sphere model with $n = 12$ in Eq. (1).⁶ In this correlation the effective potential (ϵ) relative to the thermal energy of the suspension (kT) must be increased by a large factor, determined by a Peclet number characterizing the suspension, because of the presence of the Stokes medium.

A perfect hydrodynamic medium does not thereafter alter the equations of state or the phase diagram, or affect compliance with the soft-sphere scaling laws. The reduced pressure of the soft-sphere model, for example, corresponds to the osmotic pressure of a suspension, and is defined as

$$p^* = (pV/NkT)\rho^*, \quad (2)$$

where ρ^* is the reduced hybrid density-temperature state variable⁷; for $n = 12$

$$\rho^* = (N\sigma^3/V)(\epsilon/kT)^{1/4}. \quad (3)$$

The non-Newtonian viscosity depends only upon ρ^* as

a function of an irreducible strain rate $\dot{\gamma}^*$

$$\eta^*(\rho^*, \dot{\gamma}^*) = \frac{p_{xy}^*}{\dot{\gamma}^*} = \frac{\eta\sigma^2}{(m\epsilon)^{1/2}} \left[\frac{\epsilon}{kT} \right]^{2/3} \Big|_{\rho^*, \dot{\gamma}^*}, \quad (4)$$

where p_{xy}^* is the reduced tangential stress element and the reduced strain rate is

$$\dot{\gamma}^* = \dot{\gamma}(m\sigma^2/\epsilon)^{1/2}(kT/\epsilon)^{7/12}. \quad (5)$$

For dispersions to which the soft-sphere model is applicable, Eqs. (3)–(5) show that the reduced flow curve $\eta^*(\dot{\gamma}^*)$ cannot vary independently of both reduced concentration ($N\sigma^3/V$) and reduced temperature (kT/ϵ); it depends only on the hybrid scaled product variable ρ^* . When the effective potential energy (ϵ) of typical colloidal dispersions, with $\sigma \sim 1 \mu\text{m}$, $m \sim 10^{-16}$, and medium viscosity $\eta_m \sim 1 \text{ P}$, is estimated with use of a characteristic Peclet ratio defined from Brownian motion studies,⁸

$$N_{\text{Pe}} = \frac{\eta_m \sigma^3}{kT} \left[\frac{\epsilon}{m\sigma^2} \right], \quad (6)$$

these dispersions are seen to differ from molecular fluids in that $\epsilon \gg kT$. In a statistical mechanics sense these are very low-“temperature” systems. One consequence of this drastic increase in the relative effective-potential/thermal-energy ratio is that phase transitions, which are normally associated with dense fluids and solids, may be exhibited over the whole range of dispersion dilutions. The transitions occur at characteristic ρ^* values and the low effective thermal energy can be compensated by a low concentration [Eq. (3)].

Ackerson and Clarke have reviewed the experimental literature⁹ and, further, reported light scattering studies observing a sequence of ordering transitions in a sheared dispersion with a concentration as low as 0.1%. Computer simulation studies on simple hard-sphere and soft-sphere models under conditions of homogeneous shear, in the vicinity of the freezing transitions, have also been found to exhibit a layered phase at higher strain rates.^{6,10} Since these phases

comprise two-dimensionally ordered layers of particles sliding over one another with enhanced fluidity, we shall adopt here the term “smectic” for their description.

The scaling laws for the soft-sphere ($n = 12$) model have been determined for the equilibrium fluid-crystal melting transition pressure,²

$$\tilde{p}_m = 22.6 \tilde{T}^{5/4}, \quad (7)$$

and for a glass transition from the metastable supercooled fluid to an amorphous solid,³

$$\tilde{p}_g = 53 \tilde{T}^{5/4}. \quad (8)$$

These transitions are observed in simple lyophobic dense suspensions. When $n > 6$ the bcc phases are more stable^{1,2} and freezing transitions involving both bcc and fcc/hcp phase transitions are known to occur, especially in lyophilic suspensions and charged colloidal dispersions where the effective interaction potential has a longer range.

The time-dependent ordering and disordering phenomena in sheared colloidal dispersions are a direct consequence of the applied strain rate on these transitions. Moreover, the two dominant features of the typical dense-suspension non-Newtonian steady-state flow curve, the steep shear-thinning and shear-dilatant transformations,⁶ stem from perturbations of Eqs. (7) and (8), by the applied strain rate, for freezing and glass formation.

The present results relate only to the ordering transitions and derive from computations on a model system of 512 soft spheres ($n = 12$), with homogeneously imposed shear strain, oblique periodic boundary conditions, and isothermal rescaling.¹¹ The reduced temperature for the three isochores studied is $\tilde{T} = 1.0$. Figure 1 shows the steady-state phase diagram, in the region of interest, constructed from the data points so far available. The calculations were performed by use of a variable-time-step algorithm; the data points are time averages of at least 5000 Δt corresponding to an average sample time of $\sim 10(m\sigma^2/\epsilon)^{1/2}$. Standard deviations of subaverages indicate the statistical uncertainties in single phases to be less than 1% in pressure and approximately 5% in the viscosity data.

The two-phase coexistence line drawn through the pressure points represents a shear-rate-induced reduction to the constant in Eq. (7). From $\dot{\gamma} = 0$ to $\dot{\gamma} > 0$ a discontinuity arises because the sheared crystal must exhibit plastic yield to become essentially a smectic phase in which crystal layers slide over each other. The details of the registry of the layers at low strain rates remains to be investigated. It seems reasonable to assume, however, that for a crystal to be sheared homogeneously along its most stable shearing plane (probably the 111 faces), in the limit that $\dot{\gamma} \rightarrow 0$, the thermodynamic properties of the unperturbed crystal

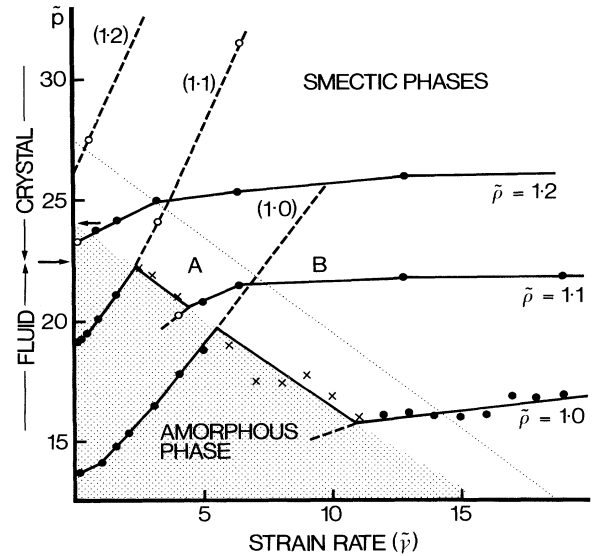


FIG. 1. Sheared soft-sphere fluid pressures. Solid points joined by solid lines denote single-phase steady-state data; dashed lines join the data (open circles) for respective metastable branches. In the single phases the statistical uncertainties are within the circle radii; data points in the two-phase regions are denoted by crosses, and for these points the errors may be as high as 5%. The arrows show the equilibrium fluid-fcc freezing transition and the amorphous-smectic coexistence line at zero strain rate.

are recovered. Shearing small periodic systems in unfavorable orientations can lead to artifacts such as shear-induced melting or other phase transitions depending on the geometry.¹²

Thermodynamic stability criteria require the crystal and fluid phases to be initially shear dilatant.¹³ The isochores in Fig. 1 show that the sheared crystal is less dilatant than the sheared fluid. At constant T, V the criterion for phase coexistence is that the partial Gibbs free energies (G) of the two phases be equal. If, when $\dot{\gamma}$ is small,

$$\left. \frac{d \Delta G}{d \dot{\gamma}} \right|_{T, V} = V \left. \frac{d \Delta p}{d \dot{\gamma}} \right|_{T, V}, \quad (9)$$

where Δ denotes the phase differences, it is clear that the effect of the shearing strain is to shift the free-energy balance in favor of the smectic crystal.

The isochores in Fig. 1 clearly show the two-phase region bounded by the commencement and completion of the shear-induced layering transition along the $p(\dot{\gamma})$ line. Within the computational uncertainties of both the data, and Eq. (7), the line extrapolates at $\dot{\gamma} = 0$ to the equilibrium fluid-crystal coexistence point.

There are several possible smectic phases. For densities below normal freezing, at low shear rate, a bcc phase is more stable than the sheared fcc/hcp phases. In the soft-sphere model the fluid-bcc and fluid-

fcc/hcp points are close together.² The sheared fluid goes first to a bcc phase, which at higher density eventually undergoes a second phase transition to one of the close-packed structures. Preliminary evidence of such a further division of the smectic phases into two regions (A and B) can be gleaned from the data in Fig. 1.

In the two-phase regions the pressure decreases with strain rate. For isothermal-isobaric shearing this would be manifested as a first-order discontinuous decrease in volume, i.e., a sharp negative dilatancy. In colloidal suspensions decreases in osmotic pressure are observed, resulting in an outflux of medium from the sheared regions and surface wetting. This effect is well known for thixotropic suspensions. It is the opposite effect of the yet more common experience of surface drying which is observed for dilatant dense suspensions, caused by a sudden increase in osmotic pressure in the sheared region,⁶ with a consequent influx of medium.

Figure 2 shows the computed rheological flow curve for the isochore $\tilde{\rho} = 1.1$. Ashurst and Hoover⁵ have given the following expression for the Newtonian

soft-sphere ($n = 12$) viscosity:

$$\tilde{\eta} \left(\frac{kT}{\epsilon} \right)^{2/3} = 0.171 + 3.025 \tilde{\rho}^4 \left(\frac{kT}{\epsilon} \right). \quad (10)$$

The Newtonian viscosities for all three isochores, obtained by extrapolating to zero-strain rate, agree, within the uncertainty ($\sim 5\%$), with Eq. (10). Confirmation of the first-order nature of the transition is obtained by the simulation of the metastable branches on both sides of the transition; both the volumetric and rheological equations of state extrapolate smoothly. Some of the metastable-phase data points are also included in Figs. 1 and 2.

The time dependence is also illustrated in Fig. 2. At a strain rate $\dot{\gamma} = 3.2$ the metastable sheared fluid branch can be observed for long times but when the strain rate is doubled to 6.4 there is a slow phase transformation to the layered phase; the non-Newtonian viscosity shear thins with a relaxation time about 10 times longer than that for responses to similar accelerations or decelerations of $\dot{\gamma}$ within either phase.

The present soft-sphere model results are compared in Fig. 3 with recent experimental measurements¹⁴ for a PVC plastisol in dioctylphthalate, chosen for its known, approximately uniform and spherical, particle distribution. The two experimental volume fractions 50% and 55% correspond closely to the soft-sphere reduced densities $\tilde{\rho} = 1.0$ and 1.1. The appropriate phenomenological reduction parameters are the New-

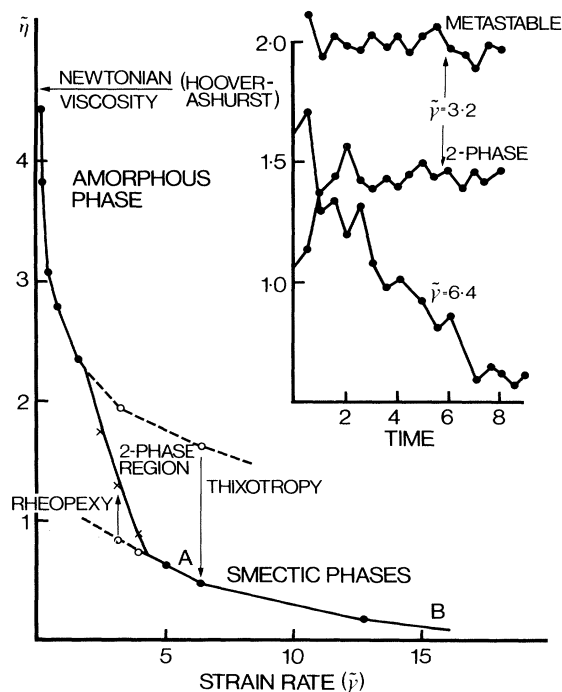


FIG. 2. Non-Newtonian viscosity of the sheared soft-sphere model for $\rho = 1.1$; solid circles, open circles, and crosses refer to stable, metastable, and two-phase points. The inset shows the time-dependent thixotropic behavior for $\dot{\gamma} = 6.4$, and both the metastability and rheopectic behavior (antithixotropy) for $\dot{\gamma} = 3.2$.

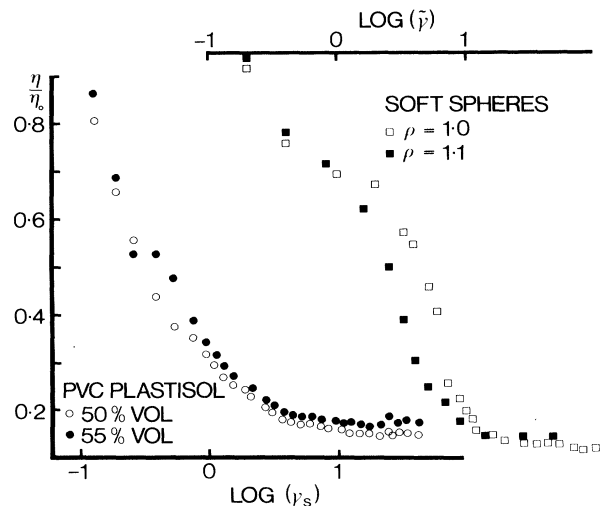


FIG. 3. A comparison with some experimental measurements of the flow curve for a suspension of PVC plastisol; the non-Newtonian viscosities are reduced according to the Newtonian values, but with original strain-rate scales in soft-sphere units and reciprocal seconds. When the strain rates are reduced (see text) the two sets of data almost coincide.

tonian suspension viscosity (η_0) and the characteristic frequency corresponding to the effective thermal energy when $\epsilon = kT$. The two sets of curves, with peculiar logarithmic strain-rate scales, almost superimpose when the plastisol values of m , σ , and ϵ [from a Peclet frequency given by Eq. (6)] are substituted to reduce the PVC strain-rate abscissa to $\log(\dot{\gamma}^*)$.

Finally, although the present studies are aimed at dense-suspension rheology, we note that the flow curves in the smectic region of Fig. 2 relate to recent investigations of sheared metallic crystals in the high-frequency domain.¹⁵ These shock-wave experiments, supported by preliminary computer simulations,¹⁶ show a square-root power-law increase in stress with shear frequency following plastic yield. If a sheared material in Couette geometry were shear strained homogeneously and isothermally, there could be no originating distinction between crystal or fluid at steady-state equilibrium. The preliminary rheological data obtained here are indicative of a complex rheogram determined by phase transitions as the relative free energies of alternative smectic phases vary with shear rate. The two-phase regions correspond to a reduction in shear stress with shear rate at constant volume. The net effect appears to be that the shear stress does not increase appreciably with shear rate but remains approximately constant to within the uncertainty of the calculations in the stability range of the smectic phases investigated. At higher strain rates large stress increases and shear thickening effects may be observed, however.⁶

Financial support from the Science and Engineering Research Council (U.K.) through the award of a Senior Research Fellowship is gratefully acknowledged. The work benefits from many helpful discus-

sions with colleagues, Professor M. F. Edwards and Dr. W. C. MacSporran.

¹W. G. Hoover, M. Ross, K. W. Johnson, D. Henderson, J. A. Barker, and B. C. Brown, *J. Chem. Phys.* **52**, 4931 (1970).

²W. G. Hoover and M. Ross, *Contemp. Phys.* **12**, 339 (1971).

³J. N. Cape and L. V. Woodcock, *J. Chem. Phys.* **72**, 976 (1980).

⁴M. Ross and P. Scholfield, *J. Phys. C* **4**, 305 (1971).

⁵W. T. Ashurst and W. G. Hoover, *Phys. Rev. A* **11**, 658 (1975).

⁶L. V. Woodcock, *Chem. Phys. Lett.* **111**, 455 (1984).

⁷For a derivation and review of the soft-sphere scaling variables see, e.g., Y. Hiwatari *et al.*, *Prog. Theor. Phys.* **52**, 1105 (1974); the distinction between hybrid state-reduced properties (asterisk) and particle reduction (tilde) is adopted here.

⁸I. M. Krieger, *Trans. Soc. Theol.* **7**, 101 (1963); see also I. M. Krieger *et al.*, *J. Colloid Interface Sci.* **34**, 16, 91 (1970).

⁹B. J. Ackerson and N. A. Clarke, *Physica (Utrecht)* **118A**, 221 (1983); a literature survey of both the equilibrium and shear-induced transition phenomena in colloidal dispersions is given in Refs. 1 to 22 of this article.

¹⁰J. J. Erpenbeck, *Phys. Rev. Lett.* **52**, 1333 (1984).

¹¹See, e.g., D. J. Evans, *Physica (Utrecht)* **118A**, 51 (1983).

¹²D. J. Evans, *Phys. Rev. A* **25**, 2788 (1982).

¹³L. V. Woodcock, *Discuss. Faraday Soc.* **76**, 334 (1983).

¹⁴M. F. Edwards, W. C. MacSporran, and L. V. Woodcock, unpublished.

¹⁵D. E. Grady, *Appl. Phys. Lett.* **38**, 825 (1981).

¹⁶W. G. Hoover, A. J. C. Ladd, and B. Moran, *Phys. Rev. Lett.* **48**, 1818 (1982).